

Post print (i.e. final draft post-refereeing) version of an article published on *Journal of Cold Regions Engineering (ASCE)*. Beyond the journal formatting, please note that there could be minor changes from this document to the final published version. The final published version is accessible from here:
[http://dx.doi.org/10.1061/\(ASCE\)0887-381X\(2007\)21:4\(121\)](http://dx.doi.org/10.1061/(ASCE)0887-381X(2007)21:4(121))
This document has made accessible through PORTO, the Open Access Repository of Politecnico di Torino (<http://porto.polito.it>), in compliance with the Publisher's copyright policy as reported in the SHERPA-ROMEO website: <http://www.sherpa.ac.uk/romeo/issn/0887-381X/>

A Cellular-Automata model for dense-snow avalanches

F. Barpi¹, M. Borri-Brunetto² and L. Delli Veneri³

¹Assistant professor, Politecnico di Torino, Department of Structural and Geotechnical Engineering, Corso Duca degli Abruzzi 24, 10129 Torino, Italy. Tel.: +39 011 090 4886. Fax: +39 090 564 4899, E-mail: fabrizio.barpi@polito.it

²Assistant professor, Politecnico di Torino, Department of Structural and Geotechnical Engineering, Corso Duca degli Abruzzi 24, 10129 Torino, Italy. Tel.: +39 011 090 4905. Fax: +39 090 564 4899, E-mail: mauro.borri@polito.it

³Consultant, Politecnico di Torino, Department of Structural and Geotechnical Engineering, Corso Duca degli Abruzzi 24, 10129 Torino, Italy.

Keywords avalanches; snow; numerical models; disasters

Abstract *This paper introduces a three-dimensional model for simulating dense-snow avalanches, based on the numerical method of Cellular Automata. This method allows one to study the complex behavior of the avalanche by dividing it into small elements, whose interaction is described by simple laws, obtaining a reduction of the computational power needed to perform a three-dimensional simulation. Similar models by several authors have been used to model rock avalanches, mud and lava flows, and debris avalanches. A peculiar aspect of avalanche dynamics, i.e., the mechanisms of erosion of the snowpack and deposition of material from the avalanche is taken into account in the model. The capability of the proposed approach has been illustrated by modelling three documented avalanches occurred in Susa Valley (Western Italian Alps). Despite the qualitative observations used for calibration, the proposed method is able to reproduce the correct three-dimensional avalanche path, using a digital terrain model, and the order of magnitude of the avalanche deposit volume.*

1 Introduction

Human activities in mountain cold regions have always been affected by the menace of snow avalanches. The location of settlements, as well as the route of trails and roads, have often been dictated by these natural phenomena, which can reach levels of extreme destructiveness. The increasing usage of land at high altitude, due to the diffusion of recreational activities and outdoor winter sports, demands for conceptual tools to be used in proper planning of infrastructures and in safe design of constructions. Engineers dealing with the problems posed by avalanche hazard need, in addition to qualitative assessments of the hydrological and geomorphological site conditions, quantitative methods to predict the effects of avalanche release. Such predictions should be based on mathematical models of the motion of falling snow masses, but the complexity of the phenomenon still defies a unified treatment of the problem along the lines of classical rational mechanics, and several approaches, with different application fields are commonly applied in practice (see [Ancey \(2001\)](#) and references therein).

Mathematical models used to describe the motion of snow avalanches are generally based on the solution of some sort of differential equation, with suitable boundary and initial conditions. A number of theories have been used to set up problems that can be solved in closed form, if simple enough, or, after discretization, by some numerical method. The reader is referred to, among others, [Hutter et al. \(1986\)](#); [Savage and Hutter \(1989\)](#); [Gray et al. \(1998\)](#); [Wieland et al. \(1999\)](#); [Tai et al. \(2001\)](#); [Iverson and Denlinger \(2001\)](#); [Denlinger and Iverson \(2001\)](#); [Wang et al. \(2004\)](#) (avalanche considered as a flow of granular material) and [Beghin et al. \(1981\)](#); [Norem et al. \(1989\)](#); [Barbolini et al. \(2000\)](#) (depth-averaged hydraulic models, where the differential equations that describe the conservation of mass and momentum are similar to the equations of fluid mechanics that characterize the motion of waves in shallow water).

In this paper, a different approach is proposed, namely one based on a inherently discrete idealization of the physical system, within the framework of Cellular Automata. The concept of cellular automata has been introduced to describe the evolution of complex systems by many Authors (for a comprehensive review see [Wolfram \(2002\)](#)), and it has been suggested as a viable alternative to the classical differential description of mathematical physics ([Toffoli, 1984](#)).

The method of cellular automata has been introduced in the modelling of rock avalanches by [Segre and Deangeli \(1995\)](#), but the antecedents of our approach can be found in a series of papers by S. Di Gregorio and co-workers ([Di Gregorio and Serra, 1999](#); [Avolio et al., 2003](#); [D'Ambrosio et al., 2003](#)). In these works, the motion of mud and lava flows, as well as of debris avalanches, has been simulated by means of cellular automata, taking into account different aspects of the physical phenomena, within a well-defined computational framework.

While some similarities can obviously be drawn between the dynamics of rock and snow avalanches, there are some peculiar aspects that characterize the evolution of a sliding snow mass, e.g. erosion of the snowpack at the front, snow entrainment, and deposition of material at the tail of the avalanche. The model presented here is a first attempt to consider the mechanisms of inclusion and deposition of snow, in a simplified yet reasonable manner, in the cellular-automata description of the avalanche, making possible the estimation of the volume of the final snow deposit.

Another important aspect to note is that the prediction of the motion of a mobilized snow mass down the slopes of a mountain is, in general, a three-dimensional problem. Although many existing mathematical models are limited to two-dimensional analyses, their application need some assumptions about the reduction of dimensionality: for instance, the choice of the trajectory of the falling mass needs to be made in advance. While in many cases this choice is reasonably easy to make, in other, more complex, topographical situations the trajectory of the avalanche can not be predicted in a trivial manner, but it should be an output of the mathematical model, as it is done here.

2 Methods

2.1 Cellular Automata

For our purposes, a cellular automaton (CA) is a mathematical representation of a physical system, whose domain is divided into simple regular parts called *cells* or *elementary automata* (EA). The *state* of a cell is a mathematical representation of some set of parameters describing its physical conditions, which can change, according to its state and to the state of other cells, belonging to the *cell neighborhood*, through a *transition function*. The state of the system is defined as the collection of the states of all the cells. It is worth noting that the state of every cell, as well as the state of the whole system, can change only at discrete time steps.

The formal definition of a cellular automaton \mathbf{A} in a d -dimensional Euclidean space is the four-tuple

$$\mathbf{A} = \langle Z^d, X, S, \sigma \rangle \quad (1)$$

where:

Z^d is the set of cells identified by integer-coordinate points in a Euclidean d -dimensional space.

X , called *neighborhood index*, is a set of m d -dimensional vectors that define the neighborhood $N(X, i)$ of cell $i = (i_1, i_2, \dots, i_d)$ according to the following rule: if $X = \{\xi_0, \xi_1, \dots, \xi_{m-1}\}$, then $N(X, i) = \{i + \xi_0, i + \xi_1, \dots, i + \xi_{m-1}\}$, where $\xi_0 =$ is the null vector.

S is the finite set of states of the elementary automaton.

$\sigma : S^m \rightarrow S$ is the transition function.

Denoting by $c(N(X, i))$ the state of the cell i as a function of its neighborhood, we define $C = \{c | c : Z^d \rightarrow S\}$ the *set of configurations* of \mathbf{A} , i.e. the set of all the possible states of the CA. Then, the *global transition function* τ (Di Gregorio and Serra, 1999) is defined as:

$$\tau : C \rightarrow C \mapsto [\tau(c)](i) = \sigma(c(N(X, i))) \quad (2)$$

Each cell is characterized by *local parameters*, which vary among the cells (e.g. centroid coordinates, cell status), and by *global parameters* that are constant for all the system (e.g. shape and size of the cells, duration of the timestep). Moreover, if necessary, an *internal transformation* may be defined, which describe the change of state of a cell based only on its state, disregarding the influence of the neighboring cells.

In general, cellular automata live in a lattice Γ , which defines also the shape of the cells. In solving physical problems, the dimension of the underlying space is usually 2 or 3.

2.2 Quasi-3D model of snow avalanches

Our cellular-automata model of snow avalanches assumes that the sliding mass is a frictional, cohesionless material (Hutter et al., 1986; Savage and Hutter, 1989, 1991; Gray et al., 1998; Wieland et al., 1999; Denlinger and Iverson, 2001; Tai et al., 2001; Wang et al., 2004). In order to keep the model as simple as possible, we use a two-dimensional cellular automaton, whose cells span a horizontal region containing the vertical projection of the zone potentially involved by the avalanche. Following Di Gregorio and Serra (1999), the third dimension, namely, the height of the avalanche profile, is one of the states of the cells. In particular, in order to respect the isotropy of motion in the horizontal plane, an hexagonal lattice with hexagonal neighborhood has been adopted (D'Ambrosio et al., 2003).

To be precise, the state of a cell is represented by the following *substates*, whose values, defined at the centroid of the cell, are assumed as representative of the entire cell (Figure 1):

H_t : *ground height*, the elevation above mean sea level of the underlying ground, which is assumed to be unaffected by the avalanche motion.

h_v : *avalanche height*, the thickness of the moving part of the avalanche.

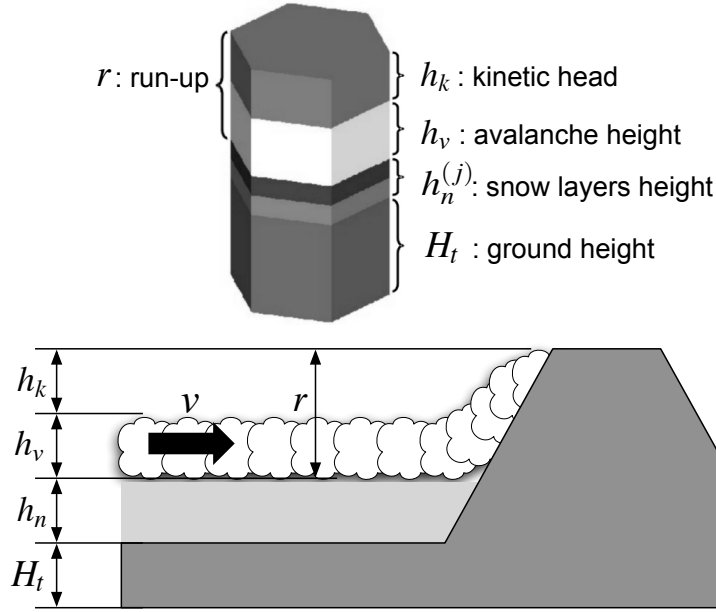


Figure 1: Definition of different *heights* (substates) for a cell, and their physical meaning.

$h_n^{(j)}$, $j = 1, n$: *snow layers height*, the thickness of the snowpack layers, which may be eroded by the avalanche.

h_k : *kinetic head*, which is a fictitious height representing the kinetic energy per unit of weight of the cell material, given by the ratio $h_k = v^2/(2g)$, where v is the velocity of the moving mass and g the acceleration of gravity.

Moreover, the sum

$$h_{\text{tot}} = H_t + \sum_j h_n^{(j)} + h_v + h_k \quad (3)$$

is called *total height* of the cell. Another important combination of the cell substates is the *run-up*, $r = h_v + h_k$, whose physical meaning is the minimum height of an obstacle needed to stop the motion of a mass with thickness h_v moving with velocity v .

The global parameters of the model are the following:

L : *cell size*, the distance between the centers of two adjacent cells, corresponding to twice the apothem of the hexagon.

T : *time step duration*, i.e., the time interval between successive upgrades of the system state.

ρ : *density of the avalanche material*. It is assumed to be constant throughout the simulation (Mellor, 1978; McClung and Schaerer, 1992; Tai et al., 2001; Sovilla and Bartelt, 2002; Bartelt et al., 2002; Sovilla, 2004).

φ : *angle of internal friction* of the avalanche material, corresponding to the repose angle of the snow.

$\rho_0^{(j)}$: *density of layer j* of the snowpack.

$p_{\text{lm}}^{(j)}$: *impact strength of layer j* of the snowpack, used to model erosion.

μ : *basal friction coefficient*.

ζ : *viscosity coefficient* of the flowing snow.

C_d : *empirical deposition coefficient*.

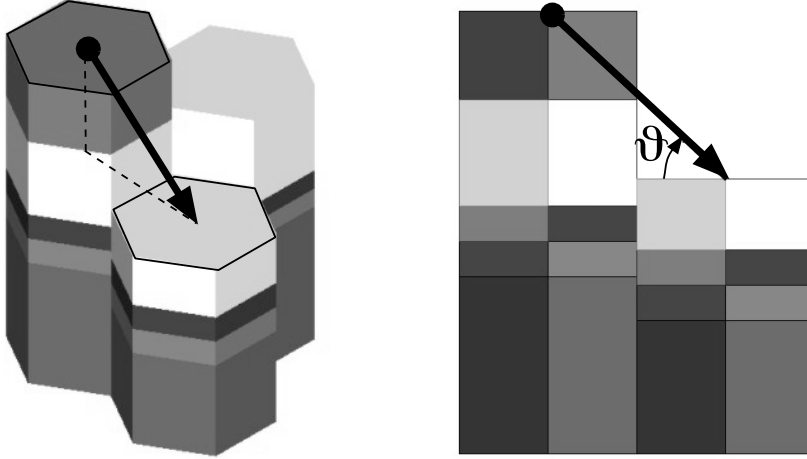


Figure 2: Slope of a fictitious incline between two adjacent cells.

The physical meaning of the friction coefficient and of the viscosity coefficient can be explained as a measure of the severity of dissipative phenomena, during the motion, the former expressing the effect of the interface towards the ground (or the resting snow), the latter introducing energy loss within the sliding snow mass. Although their well-defined physical sense, in the present paper we rather consider μ and ζ as best-fit parameters, which have to be estimated on the basis of back-analyses of the observations of real events.

The empirical deposition coefficient, C_d , is a parameter introduced in this study, and its physical meaning is defined below.

The motion of the avalanche is modeled assuming that the system, as a whole, tends to a configuration of maximum stability. This equilibrium state is attained by considering the interactions between each cell and its surrounding cells. These interactions are described in terms of incoming and outgoing flows of avalanche material to and from the neighboring cells, which, in turn, lead to variations of their height. The displacements of the avalanche material originate as a mechanism to balance the height differences among neighboring cells, and cease when these difference comes to a minimum, in a state representing the maximum equilibrium of the cells. By applying this idea to every neighborhood in the lattice, the whole system is driven to the most stable configuration by a process called *minimization of differences* (Di Gregorio and Serra, 1999).

Before applying this procedure to the avalanche model, we must exclude from flow calculations all the neighboring cells with a difference in height, with respect to the central cell, too low to induce the displacement of the material. Note that the central cell can not be excluded *a priori* from this check. If φ is the angle of internal friction of the avalanche material, the mass transfer from the central cell to cell i (in the following formulae, the cell index appears between square brackets) is possible only if the slope angle ϑ , evaluated as shown in Figure 2, is greater than φ :

$$\vartheta = \arctan \left(\frac{h_{\text{tot}}[0] - \left(H_t[i] + \sum_j h_n^{(j)}[i] + h_v[i] \right)}{L} \right) > \varphi. \quad (4)$$

Each of the remaining elementary automata is characterized by a fixed quantity, which is not distributed, given by $h[0] = H_t[0] + \sum_j h_n^{(j)}[0]$ for the central cell, and by $h[i] = H_t[i] + \sum_j h_n^{(j)}[i] + h_v[i]$, $1 \leq i < m$, for the other cells. The central cell is also given a conservative quantity $r[0] = h_v[0] + h_k[0]$, called *run-up*, that has to be distributed among the neighboring cells in order to reach the conditions of maximum stability. Let (i) $f_{\text{tot}}[i]$, $0 \leq i < m$ denote the flow going from the central cell to the neighboring cell i , (ii) $h'[i] = h[i] + f_{\text{tot}}[i]$ ($0 \leq i < m$), the sum of the fixed quantity of the cell i and the flow entering from the central cell, (iii) h'_{\min} the smallest of all the $h'[i]$. The procedure called

minimization of the differences find the flows $f_{\text{tot}}[i]$ that make minimum the following expression:

$$\sum_{i=1}^{m-1} (h'[i] - h'_{\min}). \quad (5)$$

The procedure starts from calculating the average of the quantities in the cells:

$$\bar{h} = \frac{r[0] + \sum_{i=0}^{m-1} h[i]}{m}. \quad (6)$$

The cells where the $h[i] > \bar{h}$ are excluded from further computations: no flow will be directed toward them. If not all the cells have been excluded, a new value \bar{h} is calculated, taking into account only the set of possible receivers. These two steps (calculation of the mean, and exclusion of impossible receivers) are repeated until no more cells are excluded, or, in case all the cells have been eliminated, the whole neighborhood has reached the equilibrium conditions and no redistribution is necessary. If the number of receivers is not zero, we assume that their height must increase up to the mean value \bar{h} to reach a stable configuration. In this case each receiver is given the flow

$$f_{\text{tot}}[i] = \bar{h} - h[i], \quad (7)$$

where \bar{h} is the updated mean value.

The value of $f_{\text{tot}}[i]$ is a height that represents the sum of the real height of the flowing mass and the kinetic energy, divided by the unit of weight, of the same mass. These two quantities are calculated assuming that the ratio $h_v[0]/r[0]$, evaluated before the minimization procedure, is the same for each of the outgoing flows (D'Ambrosio et al., 2003):

$$\nu = \frac{h_v[0]}{r[0]}. \quad (8)$$

According to this hypothesis, the *outgoing avalanche height flow* can be calculated as

$$f_{h_v}[i] = \nu f_{\text{tot}}[i], \quad (9)$$

and the *kinetic head flow* is given by

$$f_{h_k}[i] = f_{\text{tot}}[i] - f_{h_v}[i]. \quad (10)$$

The next step of the solution procedure requires the evaluation of the variation of the velocity of the snow mass passing from the central cell to a neighboring one. We imagine that the snow mass, in this transfer, slides on an incline, with consequent velocity increase, in case of descent ($h[i] < h[0]$), or decrease, in the opposite case ($h[i] > h[0]$). This variation is quantified by considering the energy balance of the sliding snow mass, and can be written as:

$$h_k^*[i] - h_k^*[0] = \frac{v[i]^2 - v[0]^2}{2g} = \Delta h^*, \quad i = 1, \dots, m, \quad (11)$$

where Δh^* is the elevation increment of the *centroid* of the transferred snow mass. We assume that the starting value $h_k^*[0]$ is the same for all the transfers, and depends on a mean value determined by the minimization of height differences. The destination altitude $h_k^*[i]$ is simply chosen as the material elevation of the cell i . With these assumptions we can write

$$\begin{aligned} \Delta f_{h_k} = \Delta h_k^* = & \\ & \left(H_t[0] + \sum_j h_n^{(j)}[0] + \bar{h}_v \right) - \\ & \left(H_t[i] + \sum_j h_n^{(j)}[i] + h_v[i] + \frac{1}{2} f_{h_k}[i] \right), \end{aligned} \quad (12)$$

where \bar{h}_v is the mean value of the avalanche height, obtained through the differences minimization algorithm.

As a concluding remark, we note that the time-step duration could be not enough to permit the complete transfer of the volume, expressed by eq. (7) from the central cell to each of the receiver cells. The fraction of flow that reaches its destination can be expressed by the *relaxation coefficient* (Di Gregorio and Serra, 1999; Avolio et al., 2003; D'Ambrosio et al., 2003), which is assumed to be proportional to the distance covered by the flow in a uniformly accelerated motion. After determining the increment of kinetic head by means of eq. (12), we can evaluate the distance s covered by the moving mass during a time-step, with initial velocity obtained from the kinetic head $f_{h_k}[i]$ by eq. (10). The relaxation coefficient χ is defined as the ratio of the distance s to the size of the cell, L :

$$\chi = \frac{s}{L}. \quad (13)$$

The fractions of flow, respectively of avalanche mass and kinetic energy that remain in the center cell are:

$$f_{h_v,\text{eff}}[0] = (1 - \chi)f_{h_v}[i] \quad (14)$$

$$f_{h_k,\text{eff}}[0] = (1 - \chi)f_{h_k}[i], \quad (15)$$

and the flows that are transferred to the receivers are given by

$$f_{h_v,\text{eff}}[0] = \chi f_{h_v}[i] \quad (16)$$

$$f_{h_k,\text{eff}}[i] = \chi (f_{h_k}[i] + \Delta f_{h_k}). \quad (17)$$

After updating the states of the cells, the effects of friction, erosion, and deposition are taken into account. These effects are evaluated by internal transformations alone, independently of the conditions of the neighboring cells.

2.3 Erosion mechanisms

In order to consider, in our model, the erosive phenomena, we refer to the experimental observations from in situ tests (Sovilla and Bartelt, 2002; Sovilla, 2004), which showed that the avalanche includes snow in essentially two modes: (i) *basal erosion*, due to friction forces arising between the base of the moving mass and the snowpack; (ii) *frontal erosion* (plowing), related to the impact of the leading edge of the sliding mass with the yet undisturbed snow. The second mechanism is present when the upper snow layers have a strength insufficient to withstand the action of the avalanche, which sinks below the surface.

The data reported by Sovilla (2004) show clearly that the two kinds of erosion are not quantitatively comparable: the latter is much more significant than the former. In the following developments, according to this observation, we assume that the contribution of basal erosion is negligible, and we will include in the model only the erosion process due to the frontal impact between the avalanche and the snowpack (Sovilla and Bartelt, 2002; Sovilla, 2004; Barbolini et al., 2005).

To calculate the eroded height, we assume that each cell be impacted by an equivalent flow, evaluated as the sum of all the incoming flows. If the snowpack is composed of several layers, the erosion starts from the upper one, then, if the calculated eroded depth is greater than its thickness, the layer underneath is considered, until no more plowing is required, or the snowpack is completely removed. For a given cell i , and the erodible layer j , we suppose that the avalanche flow hits an *impact area*, A , perpendicular to the ground, with width L and height \hat{h} , so that $A = L\hat{h}$. As stated before, L is cell size, and $\hat{h} = \min\{h_v[i], h_n^{(j)}[i]\}$. The impact of the avalanche leading edge on this cross-section compact the erodible layers, whose density rises from the initial value ρ_0 to a value $\rho_1 > \rho_0$, while the velocity of the erosion front u_f determines the control volume wherein the bounds between the snow particles of the erodible layers are destroyed, and they enter the avalanche. The erosion will occur only if the impact pressure p_i is larger than the strength of the layer: $p_{\text{lm}}^{(j)}$. The impact pressure, in turn, can be related to the kinetic head by the relationship

$$p_i = 2\rho g c_i h_k[i], \quad (18)$$

where c_i is a shape factor.

By applying to the control volume the theory by [Sovilla \(2004\)](#), the front velocity can be expressed during the time-step T as

$$u_f = \sqrt{\frac{p_i}{\rho_0 \left(1 - \frac{\rho_0}{\rho_1}\right)}}, \quad (19)$$

and the eroded depth is found to be:

$$h_n = u_f \frac{\rho_0}{\rho} T. \quad (20)$$

where:

ρ_0 : density of the snow layer before impact

ρ_1 : density of the snow layer after impact

u_f : front velocity, which can be assumed equal to the avalanche velocity, v

T : time-step duration.

The calculations are repeated for all the erodible layers in the snowpack, until either the eroded depth is smaller than the layer thickness, or the whole snowpack has been eroded.

2.4 Deceleration due to friction and viscosity

The kinetic head of a cell may be reduced, during a time-step, because of basal friction and viscosity. For an avalanche mass contained in the cell i sliding on a horizontal plane, the velocity decrement is given by ([Bartelt et al., 2002](#); [Sovilla and Bartelt, 2002](#); [Sovilla, 2004](#)):

$$\Delta v = \left(\mu + \frac{h_k[i]2g}{\zeta h_v[i]} \right) gT, \quad (21)$$

where μ is the *basal friction coefficient* and ζ is the *coefficient of viscosity*.

These parameters lack of a true physical meaning, and may be used, together with the empirical deposit coefficient C_d , to perform the *calibration* of the model. This procedure consists in simulating well-documented events to define a suitable combination of parameters. It must be pointed out that a similar procedure is used by other researchers, see, for instance, [Bartelt et al. \(2002\)](#); [Sovilla \(2004\)](#).

If at the beginning of a time step the velocity in the cell i is $v = \sqrt{2gh_k[i]}$, the updated kinetic head can be written as

$$h_k^*[i] = \frac{(v - \Delta v)^2}{2g}, \quad (22)$$

where the decrement in velocity Δv is given by eq. (21). Of course, the kinetic energy can not be negative, so that if the value obtained from eq. (22) is lower than zero, the assumption $h_k^*[i] = 0$ is made.

2.5 Deposition

We assume that the deposition of material is possible only when its kinetic energy falls below a limit threshold. For a given cell, during a time step, the mass of the deposited material will be proportional to the difference between the kinetic head of the cell (evaluated after the consideration of frictional and viscous effects) and a limit kinetic head, $h_{k,\text{lim}}$.

The deposition of the avalanche material will occur only if $h_k[i] < h_{k,\text{lim}}$. The height of the deposit is assumed to be

$$h_d = C_d \frac{h_{k,\text{lim}} - h_k[i]}{h_{k,\text{lim}}} h_v, \quad (23)$$

where C_d (coefficient of deposition) and $h_{k,\text{lim}}$ are empirical parameters.


```

begin
  Read input data;
  Assign the initial state of the cells;
  repeat
    increment time;
    forall the cells in the lattice do
      Determine the global indices of neighboring cells;
      Evaluate the outgoing flows (minimization of differences);
      Calculate the relaxation coefficient  $\chi$ ;
      forall the cells in the neighborhood do
        Calculate effective flows in this timestep;
        Assign flows to that cell (global index);
      end
    end
    forall the cells in the lattice do
      Sum the incoming flows;
      Evaluate erosion;
      Calculate kinetic energy loss (friction and viscosity);
      Calculate deposition;
    end
  until the state of the system becomes stationary ;
end

```

Figure 3: Main steps of the solution procedure.

2.6 Solution algorithm

Figure 3 summarizes the main steps of the procedure, which has been coded in a C language program, called ASCA (Avalanche Simulator through Cellular Automata), that implements the concepts presented above.

3 Observations

In order to calibrate the best-fitting parameters of the numerical model ASCA, described in the previous section, we have chosen three avalanches observed in the Susa Valley (Western Italian Alps). These events differ in some aspects of their initial conditions and their evolution, allowing response of the model to be tested in diverse situations. In this section, to make possible the comparison of the results obtained by simulation, a brief description of the main features of each event is given.

The description of the avalanches (thickness of snow cover, snow conditions, geometry of the fracture zone, etc.) have been provided by the *Consorzio Forestale Alta Valle Susa* (Upper Susa Valley Forest Authority). We wish to remark that these data are not obtained from observations on instrumented sites, but represent mainly *qualitative records* of recurring events potentially affecting important infrastructures (highways and ski resorts).

3.1 Mount Jafferau avalanche

The first case we present here is the avalanche fallen from the southern flank of Mount Jafferau on January 5, 2004 (see the main data in Table 1).

The event was described by an eyewitness as a cloud avalanche, which does not fall in the class of phenomena described by the model presented in this paper. Nevertheless, we choose to analyze this case because of the relative simplicity of the topographical conditions, to focus the attention on the influence on the results of the other physical parameters.

The path of the avalanche, as shown from the shaded zone in Figure 4, is generally in the maximum dip direction (South-East), but followed a gentle depression in the topography, along a small gully. The presence of this groove, and its influence on the phenomenon is discussed below, commenting the results obtained from the simulation.

Table 1: Description of the observed avalanches.

Characteristic	Mt. Jafferau	Chanteloube Creek (S) ^a	Chanteloube Creek (D)
Date	Jan. 5, 2004	Dec. 10, 1996	Feb. 6, 1994
Position	45°04'49"N, 6°46'06"E	45°04'32"N, 6°50'38"E	45°04'24"N, 6°50'34"E ^b
Crown elevation (m)	2700	2300	2080
Avalanche type	loose-snow	wet loose-snow	loose-snow
Snow type	dry, low cohesion	wet, low cohesion	dry, low cohesion
Bed surface	snow interface	ground	ground
Slab thickness (m)	0.5	1.5	1.3
Slab width (m)	150	—	200
Snow thickness (m)	2.0	1.5	1.3
Terminus elevation (m)	2210	1100	1080
Length of path run (m)	470	1900	2280
Deposit length (m)	300	70	150
Deposit width (m)	60	12	120
Deposit thickness (m)	3	5	9
Deposit volume (m ³)	10 000	4200	30 000

^a Two events were recorded in the site of Chanteloube Creek: a single path avalanche (S), and a double path avalanche (D).

^b Data for the first release zone. The second release zone is the same of case (S).

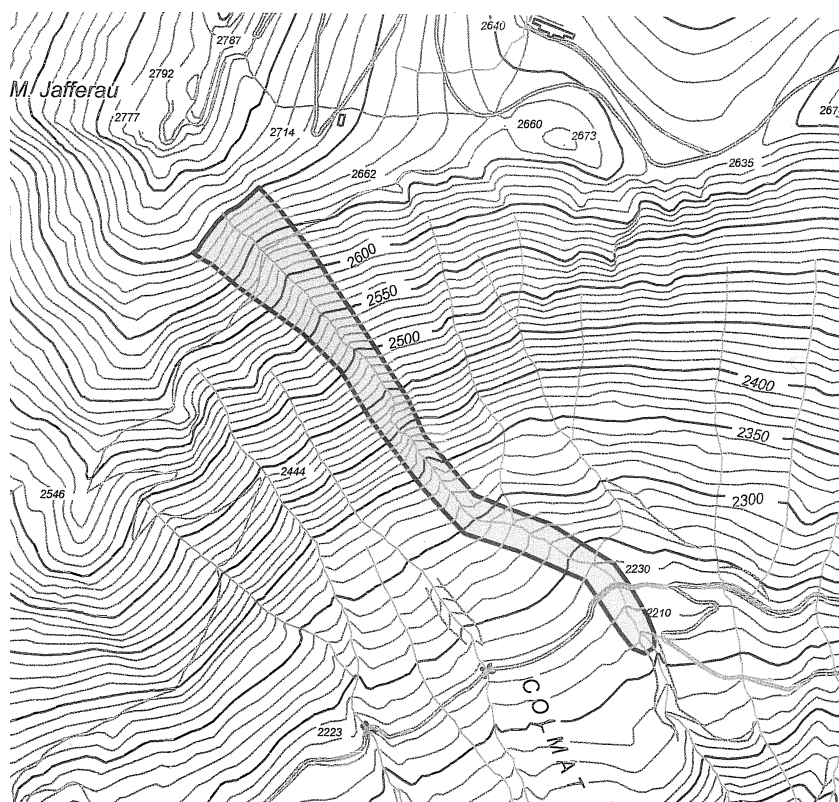


Figure 4: Site of Mt. Jafferau avalanche (Jan. 5, 2004). The shaded zone represents the path of the avalanche, which follows a creek that does not show up in the DEM.

Table 2: Parameters and best-fit results of the simulations.

Characteristic	Mt. Jafferau	Chanteloube Creek (S)	Chanteloube Creek (D)
Lattice size (cells)	250×270	440×530	440×530
Cell apothem L (m)	2.5	2.5	2.5
time-step duration T (s)	0.1	0.1	0.1
Number of steps	3882 (3200)	4000	5616
Sliding friction parameter μ	0.006	0.002327	0.002327
Viscosity parameter ζ (ms^{-2})	200	1028	1028
Deposit coefficient C_d^a	—	0.25	0.5
Deposit length (m)	237	98	110
Terminus elevation (m)	2220	1080	1080
Deposit width (m)	127	65	75
Deposit thickness (m)	3	9	12
Estimated volume (m^3)	42 790	25 164	80 981

^a Erosion and deposition mechanisms are not considered in simulations of Mt. Jafferau avalanche.

3.2 Chanteloube Creek single avalanche

The second event is the avalanche of Chanteloube Creek of December 10, 1996. It is a small channeled avalanche, which follows a marked couloir in South-East direction. The snow was wet, with low cohesion (see Table 1, case (S)). The path was nearly 2 km long, with a difference in height of 1.2 km, and the motion stopped at the toe of the slope, on an almost horizontal surface.

3.3 Chanteloube Creek double avalanche

The last event is the avalanche in the site of Chanteloube Creek that occurred on February 6, 1994. In this case, two starting zones, each one in a different branch of the creek, have been observed (Table 1, case (D)). We lack of specific information on the temporal evolution of the phenomenon, and some assumptions need be made to simulate the observed final situation.

4 Application

In this section, we present the results obtained by simulating with the numerical code ASCA, the three avalanches described above. The characteristics of the simulations (cell size, time-step duration, mechanical parameters, etc.) have been chosen according to the particular event (snow density, cohesion, etc.), to the comparison of simulated and observed results, and, when other suggestion were missing, simply to common sense. The description of the terrain used in the modeling is given by the Digital Elevation Model (50 m horizontal resolution) produced by *Regione Piemonte* (Piedmont Region).

4.1 Mount Jafferau avalanche

The simulation presented here has been obtained neglecting the erosion and deposition mechanisms. The values of the parameters μ and ζ , considered as best-fitting parameters, have been adjusted in order to obtain a good approximation of the terminus position. The main results are reported in Table 2, while a pictorial representation of the final state of the avalanche is shown in Figure 5.

A comparison of the simulated results to the observations shows that the numerical model predicts an almost rectilinear trajectory, and a wider snow mass involved in the phenomenon. In this case, the discrepancy can be imputed to the lack of resolution of the digital terrain used in simulations. In fact, as can be seen in Figure 4, the real avalanche follows a small ditch, whose cross section is too small to appear in the digital terrain, defined only by the elevation at the grid-points, with spacing of 50 m. Also, the larger width of the calculated deposit zone can be ascribed to the same cause: in

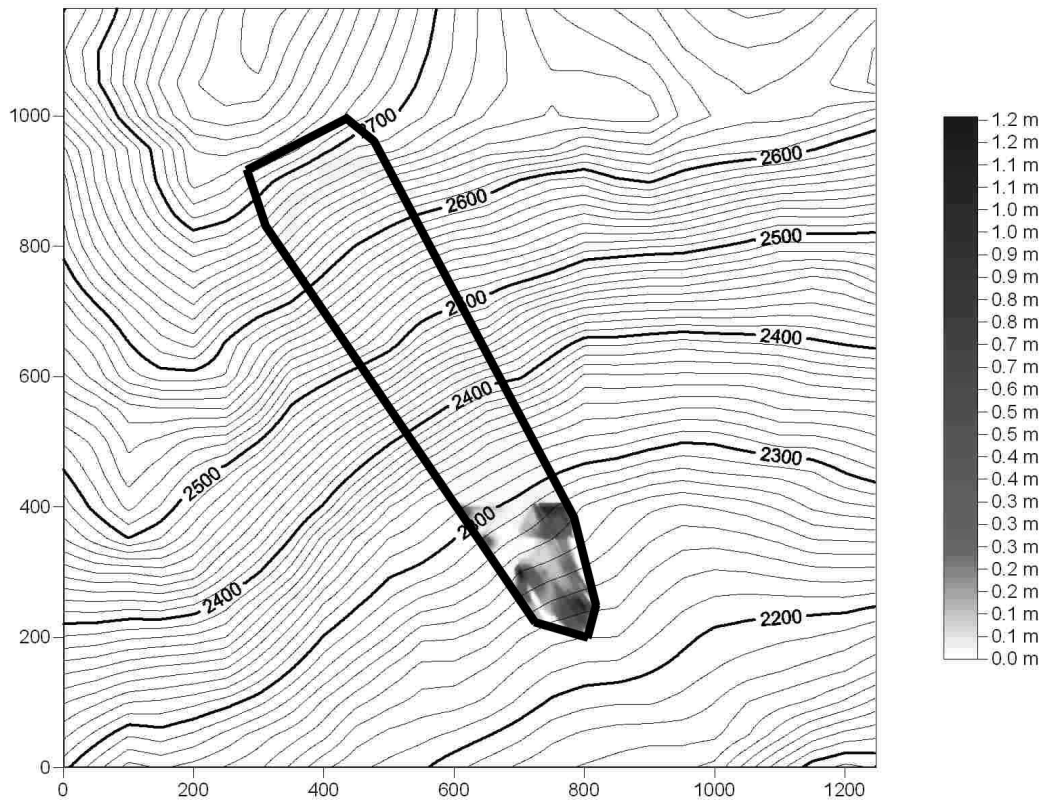


Figure 5: Mt. Jafferau avalanche simulation: position of the avalanche material at the end of the simulation. The thickness of the material is represented by the grey scale, and the thick line shows the area affected by the avalanche.

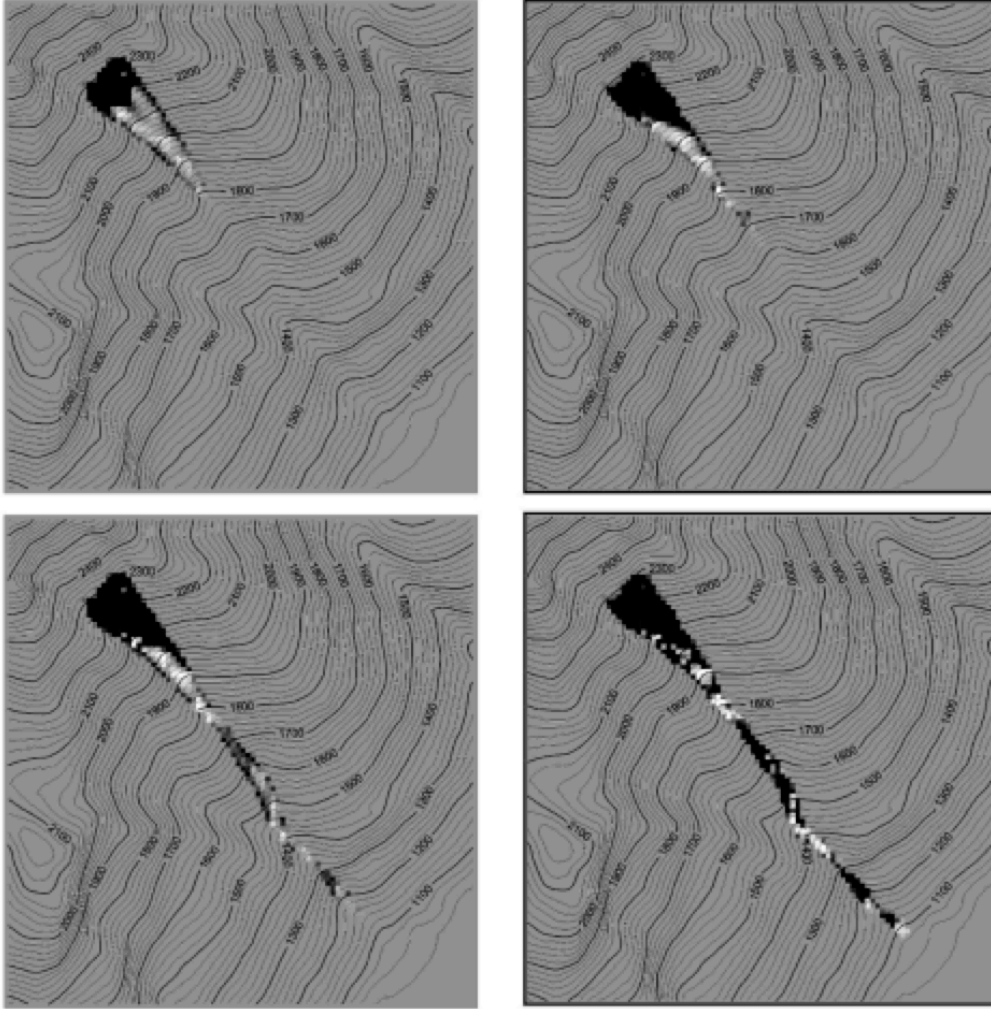


Figure 6: Chanteloube creek (case S): eroded zones are black, deposition zones are white.

the model the avalanche flow is substantially unconfined, and tends to expand to a larger area. In the calculation of the deposit volume, also the snow cover has been considered, so that a larger deposition area corresponds to a volume larger than that estimated from the observations. All things considered, we want also emphasize that ASCA is able to produce a satisfactory simulation of the Mount Jafferau avalanche: the affected zone, the terminus elevation, and the thickness of the deposited material can be calculated with sufficient precision. Although the model is conceived to model dense-snow flowing avalanches, even in this case it yields fair results.

4.2 Chanteloube Creek single avalanche

The simulation of the Chanteloube Creek avalanche produced quite realistic results summarized in Table 2, while in Figure 6 the evolution of the phenomenon is presented, through four successive configurations of the avalanche. In these pictures, the original snow cover is depicted in intermediate gray, while the eroded zones are black and the intensity of white is related to the thickness of the avalanche. As in the previous case, it can be noted that the calculated area of the deposit zone is overestimated by the calculations, both width and length are greater than the in situ measurements, and so the calculated volume is much bigger than the estimated one. This drawback is compensated by the correct determination of the avalanche path, and the effectiveness of the simulation of erosion and deposition mechanisms.

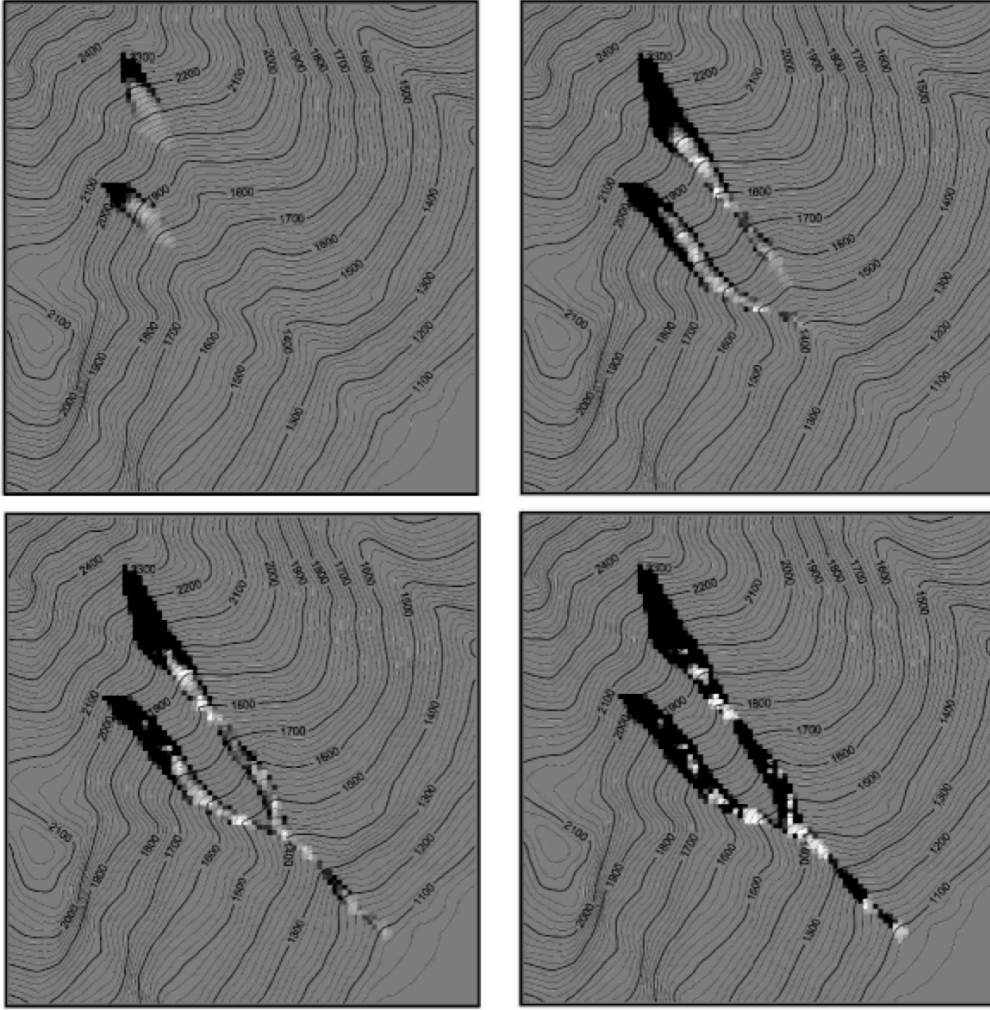


Figure 7: Chanteloube creek (case D): eroded zones are black, deposition zones are white.

4.3 Chanteloube Creek double avalanche

The complete avalanche run has been simulated using 5616 steps, each one spanning 0.1 s, noting that no appreciable variations in the configuration of the system could be detected after the 4500th step. The parameters obtained by best fitting are summarized in Table 2, and four snapshots of the simulated avalanche motion are presented in Figure 7. In Figure 8 a three-dimensional view of the same data is depicted.

5 Discussion

The simulation presented in the paper, even if they can not be considered as an exhaustive study that allows the calibration of the model, show that ASCA is able to obtain interesting results. The comparisons between simulation results and real observations are encouraging. In particular, the study of the avalanche of Chanteloube Creek gave good results in evaluating the avalanche path, and the erosion of the snowpack. The differences from the observed results are, in general, on the conservative side. For instance, the evaluation of the deposit area and volume gave values larger than the real ones, yet with the correct order of magnitude.

On the other hand, in the case of Mount Jafferau avalanche, the simulations showed up more difficulties. First of all, the modeling mechanisms of erosion and deposit, which gave bad results, had to be excluded. Also, only a rough prediction of the avalanche path was obtained, even if the correct

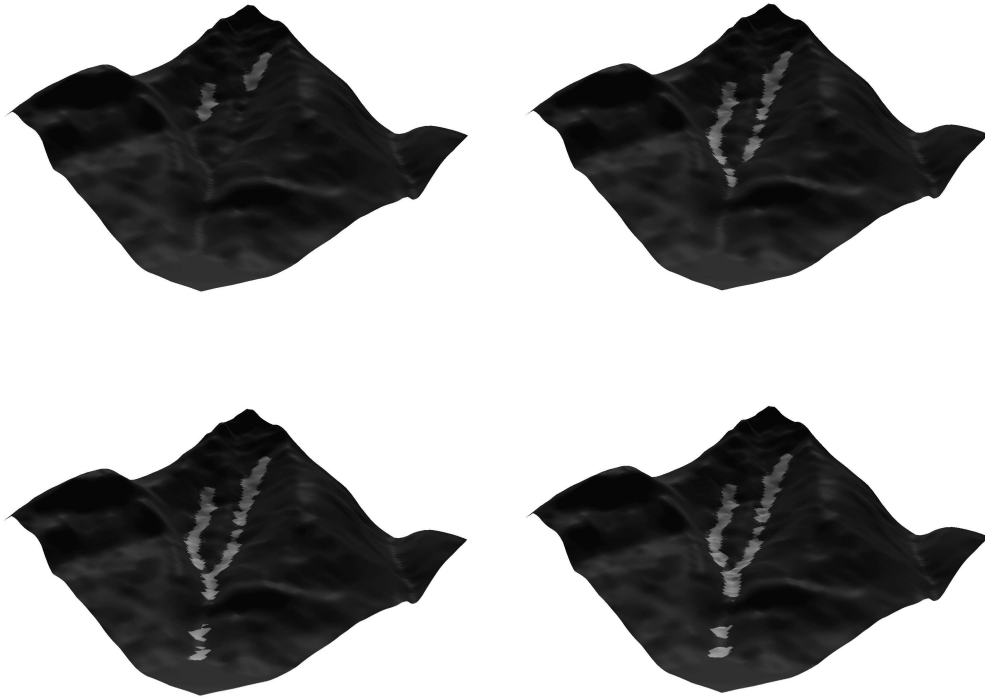


Figure 8: Chanteloube creek (case D): three-dimensional depiction.

value of the total run-out distance was imposed through trial and error. The origin of this drawback is found in the insufficient resolution of the terrain model used in the simulation. In fact, the real avalanche followed a ditch whose size was too small to appear in the 50 m resolution DEM. Moreover, an important limit of ASCA is implied in its formulation, namely the lack of a proper consideration of the aerosol phase in the model, probably present in the real event. An evolution of the proposed model to include the aerosol phase should be possible, along the lines of [Crisci et al. \(2005\)](#), where a pyroclastic flow has been modeled.

The most important problem that emerged in the application of ASCA is a not well-defined relationship between the simulated duration of an event, and the size of the cells. In fact, we observed that by reducing the cell size, the final, motionless configuration of the system is attained with a larger number of steps (keeping fixed the time-step duration). The nature of this mesh dependency has not yet been clarified, and as a consequence, the calculation of the velocity and of the derived quantities is at least questionable. In order to quantify the magnitude of this effect in different situations, it seems necessary a deeper analysis, by comparing the results from other models or, better, with experimental data from well-documented avalanche events.

To summarize a possible usage of ASCA, the application of the proposed method at a given site could be conducted through the following steps.

- The site topography (digital terrain model), an average value of snow density and the number and thickness of snowpack layers are assumed to be known with sufficient accuracy.
- A best-fitting, by a trial and error procedure, of μ , ζ and C_d for different snow and boundary conditions trying to match the main features of observed events is carried out. These parameters are used in subsequent numerical simulations.
- The envelope of possible deposit zone, path and run-out distance is obtained varying, for instance, the position and geometry of the starting zone, and snow entrainment.

- The results in terms of run-out distances and deposit volume can be used for zoning purposes and design of snow dams and deviators.

6 Conclusion

The cellular-automata model presented here for the simulation of snow avalanches is a novel method presenting interesting capabilities. The simulations of real events show that accurate results can be obtained very quickly, with inexpensive hardware. The numerical model can cope with the full three-dimensional topography of many real situations, as described by sufficiently accurate digital terrain models, potentially overcoming a major drawback of many existing approaches to avalanche simulation.

It should be emphasized that the contribution of the paper is methodological, and it is not intended to be a research devoted to find the best parameters necessary for the simulations of events on a specific site (the data employed are not sufficiently accurate for such a purpose). Much work remains to do, both on the calibration of the model and on the model itself, as explained at the end of the Discussion section.

Acknowledgment

The authors wish to thank L. Caffo and A. Dotta of *Consorzio Forestale Alta Valle Susa (CFAVS)* for providing the data from the in situ observations.

References

- Ancey, C. (2001). “Snow avalanches.” *Geomorphological fluid mechanics*, N. J. Balmforth and A. Provenzale, eds., Vol. 582 of *Lecture Notes in Physics*, Springer Verlag, 319–338.
- Avolio, M. V., Crisci, G. M., D’Ambrosio, D., Di Gregorio, S., Iovine, G., Rongo, R., and Spataro, W. (2003). “An extended notion of cellular automata for surface flows modelling.” *WSEAS Trans. Comp.*, 2, 1080–1085.
- Barbolini, M., Biancardi, A., Cappabianca, F., Natale, L., and M. Pagliardi (2005). “Laboratory study of erosion processes in snow avalanches.” *Cold Reg. Sci. Technol.*, 43, 1–9.
- Barbolini, M., Gruber, U., Keylock, C., Naaim, M., and Savi, F. (2000). “Application of statistical and hydraulic-continuum dense-snow avalanche model to five real European sites.” *Cold Reg. Sci. Technol.*, 31, 133–149.
- Bartelt, P., Christen, M., Gruber, U., and Filaferro, E. (2002). “AVAL-1D: an avalanche dynamics program for the practice.” *Proc. of Interpraevent 2002 in the Pacific Rim*, Vol. 2, Matsumoto, Japan. Int. Res. Soc. Interpraevent for the Pacific Rim, 715–725.
- Beghin, P., Hopfinger, E., and Britter, R. (1981). “Gravitational convection from instantaneous sources on inclined boundaries.” *J. Fluid Mech.*, 107, 407–422.
- Crisci, G. M., Di Gregorio, S., Rongo, R., and Spataro, W. (2005). “PYR: a Cellular Automata model for pyroclastic flows and application to the 1991 Mt. Pinatubo eruption.” *Future Gener. Comp. Sy.*, 21, 1019–1032.
- D’Ambrosio, D., Di Gregorio, S., and Iovine, G. (2003). “Simulating debris flows through a hexagonal cellular automata model: Sciddica $S_{3\text{-hex}}$.” *Nat. Hazard Earth Sys.*, 3, 545–559.
- Denlinger, R. P. and Iverson, R. M. (2001). “Flow of variably fluidized granular masses across three-dimensional terrain. 2. Numerical predictions and experimental tests.” *J. Geoph. Res.*, 106(B1), 553–566.
- Di Gregorio, S. and Serra, R. (1999). “An empirical method for modelling and simulating some complex macroscopic phenomena by cellular automata.” *Future Gener. Comp. Sy.*, 16, 259–271.
- Gray, J. M. N. T., Wieland, M., and Hutter, K. (1998). “Gravity-driven free surface flow of granular avalanches over complex basal topography.” *Proc. R. Soc. A*, 455, 1841–1874.
- Hutter, K., Szidarovszky, F., and Yakowitz, S. (1986). “Plane steady shear flow of a cohesionless granular material down an inclined plane: a model for flow avalanches.” *Acta Mech.*, 63, 87–112.
- Iverson, R. M. and Denlinger, R. P. (2001). “Flow of variably fluidized granular masses across three-dimensional terrain. 1. Coulomb mixture theory.” *J. Geoph. Res.*, 106(B1), 537–552.
- McClung, D. and Schaerer, P. (1992). *The avalanche handbook*. The Mountaineers, Seattle, Washington.
- Mellor, M. (1978). “Dynamics of snow avalanches.” *Rockslides and Avalanches, 1: Natural Phenomena*, B. Voight, ed., Vol. 14A of *Developments in Geotechnical Engineering*, Elsevier Scientific, New York, 753–792.
- Norem, H., Irgens, F., and Schieldrop, B. (1989). “Simulation of snow-avalanche flow in run-out zones.” *Ann. Glac.*, 13, 218–225.
- Savage, S. B. and Hutter, K. (1989). “The motion of a finite mass of granular material down a rough incline.” *J. Fluid Mech.*, 199, 177–215.

- Savage, S. B. and Hutter, K. (1991). “The dynamics of avalanches of granular materials from initiation to runout.” *Acta Mech.*, 86, 201–223.
- Segre, E. and Deangeli, C. (1995). “Cellular automaton for realistic modelling of landslides.” *Nonlin. Proc. Geoph.*, 2, 1–15.
- Sovilla, B. (2004). “Field experiments and numerical modelling of mass entrainment and deposition processes in snow avalanches,” PhD thesis, Swiss Federal Institute of Technology, Zurich.
- Sovilla, B. and Bartelt, P. (2002). “Observation and modelling of snow avalanche entrainment.” *Nat. Hazards Earth Sys. Sci.*, 2, 169–179.
- Tai, Y. C., Hutter, K., and Gray, J. M. N. T. (2001). “Dense granular avalanches: mathematical description and experimental validation.” *Geomorphological fluid mechanics*, N. J. Balmforth and A. Provenzale, eds., Vol. 582 of *Lecture Notes in Physics*, Springer Verlag, 339–366.
- Toffoli, T. (1984). “Cellular automata as an alternative to (rather than an approximation of) differential equations in modeling physics.” *Physica D*, 10, 117–127.
- Wang, Y., Hutter, K., and Pudasaini, S. P. (2004). “The Savage-Hutter theory: a system of partial differential equations for avalanche flows of snow, debris and mud.” *ZAMM*, 84, 507–527.
- Wieland, M., Gray, J. M. N. T., and Hutter, K. (1999). “Channelized free-surface flow of cohesionless granular avalanches in a chute with shallow lateral curvature.” *J. Fluid Mech.*, 392, 73–100.
- Wolfram, S. (2002). *A new kind of science*. Wolfram media Inc., Champaign.